*International Journal of Fracture* **92:** 271–285, 1998.

# Development of a process zone in rubber-modified epoxy polymers

J. DU[1], M.D. THOULESS[1,2] and A.F. YEE[1]
[1]*Department of Materials Science and Engineering, The University of Michigan, Ann Arbor, Michigan 48109, USA. e-mail: jgdu@engin.umich.edu afyee@engin.umich.edu.*
[2]*Department of Mechanical Engineering and Applied Mechanics, The University of Michigan, Ann Arbor, Michigan 48109, USA. e-mail: thouless@engin.umich.edu.*

Received 30 May 1997; accepted in revised form 28 July 1998

**Abstract.** The effects of a process zone on toughness and on $R$-curve behavior were investigated for a model, rubber-modified epoxy polymer. The system studied was one in which the bridging mechanism of toughening does not operate. The characteristic features of $R$-curve behavior, a rise in toughness with crack extension until an approximate steady-state is reached, were observed using double-cantilever-beam tests. The evolution of the process zone was studied using transmission-optical microscopy. As the crack grew, the process zone appeared to fan out until it reached a steady-state thickness; it then remained a uniform size upon further crack advance. The features of the experimental $R$-curves were shown to be directly correlated to the evolution of the process zone. Furthermore, the effect of the portion of the process zone in the crack wake was examined by a series of experiments in which the wake was partially removed, and the $R$-curve re-established by subsequent loading. These experiments demonstrated that removal of the crack wake caused the crack-growth resistance to drop. The toughness then built back up to the steady-state value as the crack wake re-developed. This unambiguously demonstrated a contribution to toughening from the crack wake despite the absence of any observable bridging mechanism. These results support the accepted notion that an extrinsic toughening mechanism is responsible for the increased toughness observed upon adding rubber particles to an epoxy matrix

**Key words:** Rubber-modified, epoxy, fracture, $R$-curve, process zone, toughness, crack wake.

## 1. Introduction

Materials such as ceramics and highly-cross-linked polymers are intrinsically brittle because their cohesive strength is relatively low compared to the stress required to initiate dissipative processes in the crack-tip region (Tvergaard and Hutchinson, 1992). These materials can frequently by toughened by the addition of a second phase that triggers inelastic processes at a much lower stress. There has been much work on understanding this mechanism of toughening, where energy is absorbed by nonlinear deformation in a process zone surrounding the crack but macroscopic deformation is dominated by linear elasticity (McMeeking and Evans, 1982; Budiansky et al., 1983; Evans and Faber, 1984).

It has been shown that the toughness of such materials is very sensitive to the size and shape of the process zone (Tvergaard and Hutchinson, 1992; McMeeking and Evans, 1982; Budiansky et al., 1983; Evans and Faber, 1984). In particular, material within the process zone does not contribute to an enhanced toughness if it has experienced only a monotonically increasing strain. Toughening does not occur simply by triggering nonlinear stress-strain behavior ahead of a crack, even if this is associated with a process that dissipates energy. The material in the process zone must undergo some reversal in strain if this energy dissipation is to manifest itself as an increased driving force being required for crack propagation. As a result, when a crack

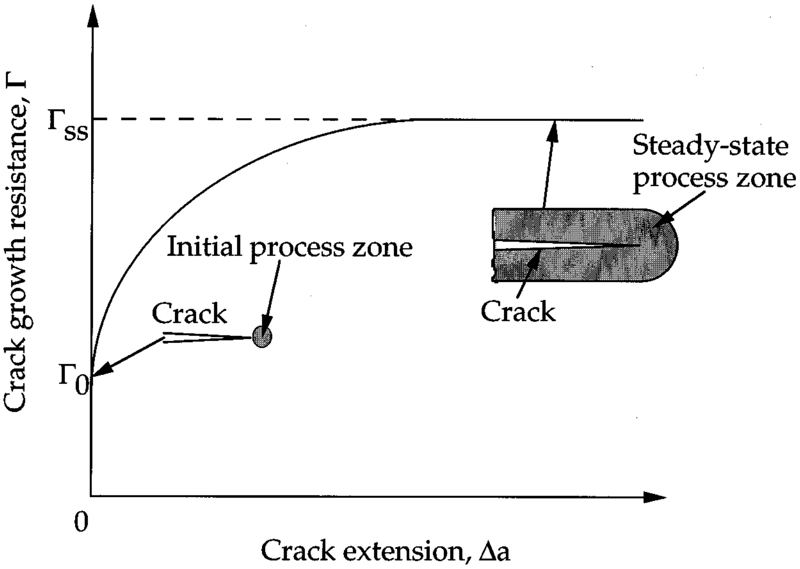

*Figure 1.* Schematic diagram of a typical $R$-curve for toughened brittle materials. $\Gamma_0$ is the initial toughness, and $\Gamma_{ss}$ is the steady-state toughness.

grows into a process zone that has been established ahead of it, the energy-release rate required to grow the crack will gradually increase from an initial value close to the intrinsic toughness of the material, $\Gamma_0$. This increase in toughness with crack length is known as $R$-curve behavior (Figure 1). It should be noted that the existence of an $R$-curve is a necessary corollary to any *extrinsic* toughening mechanism in which a nonlinear process zone is embedded within a linear-elastic matrix (Tvergaard and Hutchinson, 1992). The absence of an $R$-curve for a material would indicate that fracture is governed only by the *intrinsic* toughness (representing the energy absorbed by the decohesion process itself). In other words, extrinsic models of toughening, in which energy absorption occurs in a process zone around the crack tip, would be inappropriate. Any changes in toughness that were observed by modifying the material would have to be ascribed to a change in the actual decohesion process itself. Conversely, the existence of an $R$-curve indicates that extrinsic toughening mechanisms with a process or/and a bridging zone are significant.

An extrinsic toughening mechanism results in a toughness of the form

$$\Gamma = \Gamma_0 + \Delta\Gamma, \tag{1}$$

where $\Delta\Gamma$ is a function of a crack length and represents the local contribution of all sources of extrinsic toughening. As a crack grows, the region of high stress associated with the crack tip advances and extends the process zone. At the same time, material that is already in the process zone is unloaded as the crack advances beyond it. Ultimately, when the crack has advanced sufficiently far, a steady-state cycle will be reached where the volume of material entering the process zone ahead of the crack is equal to the volume of material that is completely unloaded in the crack wake. At this point, the measured toughness is independent of crack length (Tvergaard and Hutchinson, 1992). Under these conditions, the steady-state extrinsic toughening is given by

$$\Delta\Gamma_{ss} = 2\int_0^h U(y)\,\mathrm{d}y, \tag{2}$$

where $h$ is the size of the process zone, and $U(y)$ is the area traced out by the stress-strain curve for an element situated at a distance $y$ from the crack plane as it moves from a region far ahead of the crack tip to an unloaded state in the crack wake.

Micromechanics modeling of the toughening mechanisms of rubber-modified epoxies are all based on the assumption that a process zone exists around a crack tip. Furthermore, it is always assumed that this process zone is embedded in a linear-elastic region, and that linear-elastic fracture mechanics (L.E.F.M.) can be used to characterize fracture and to measure the toughness. (This means that the macroscopic response of the cracked material is dominated by linear-elasticity.) Therefore, these models are described exactly by the mechanics discussed above. As the crack tip advances, material ahead of the crack experiences nonlinear deformation that absorbs energy. This is expressed as an enhanced toughness as the material passes through the process zone into the wake of the crack and is unloaded. In ceramic materials, this nonlinear process may occur by phase transformations or microcracking (McMeeking and Evans, 1982; Budiansky et al., 1983; Evans and Faber, 1994; Knehens and Steinbrech, 1982; Swain and Hannink, 1984; Marshall and Swain, 1988; Rose and Swain, 1988; Yu and Shetty, 1989) (in addition to any bridging caused by grain pull-out (Swanson et al., 1987)). In rubber-modified epoxies, it is well established that energy absorption occurs by cavitation of the rubber particles and subsequent shear deformation of the matrix (Kinloch et al., 1983a,b; Yee and Pearson, 1986; Pearson and Yee, 1986; Huang and Kinloch 1992; Evans et al., 1986). (With large enough particles, crack bridging may also occur (Kunz-Douglass et al., 1980).)

While these models have generally been discussed in the polymers literature in terms of the events that occur ahead of the crack tip, the quantitative results are formulated as in Equation 2 (Huang and Kinloch, 1992; Evans et al., 1986; Kinloch and Guild, 1996). Furthermore, it should be appreciated that since these models assume extrinsic mechanisms of toughening by energy absorption, an $R$-curve type of behavior must be expected if they are correct. The absence of $R$-curve behavior would cast doubt on the validity of these established models, and would suggest instead that the origin of the toughening in these materials resides in a change in the intrinsic toughness, perhaps associated with a change in the actual decohesion mechanism itself. Given the general acceptance of the process-zone models for rubber-toughened epoxies, it is therefore somewhat strange that the existence of $R$-curves have not been established for these materials[1].

The work described in this paper was conducted to examine $R$-curve behavior and the effects of the crack wake on toughness for a rubber-modified epoxy polymer. CTBN-toughened DGEBA epoxies were chosen as the model system. Because of high solubility in DGEBA epoxies, CTBN rubber forms relatively fine particles (diameters of about 0.2–2 $\mu$m depending on the acrylonitrile content and the epoxy system) with a narrow size distribution. Previous work indicates that no bridging mechanisms operate at an observable scale in these materials (Pearson and Yee, 1991). Double-cantilever-beam tests were performed to observe the evolution of the process zone, and to obtain the $R$-curves of epoxies toughened by different quantities of the rubbery phase. Several microscopy techniques were employed to examine the nature of the fracture surfaces and the process zones in these materials. The effect of

---

[1] Generally, $R$-curve studies in the polymers literature have focused on tough polymers with a high ductility (Hashemi and Williams, 1991; Zhou et al., 1994; Crouch and Huang, 1994). This ductility gives rise to crack blunting and tearing events associated with extensive plasticity. If the nonlinear zone occupies a substantial portion of the specimens, the requirements of linear-elastic fracture mechanics (L.E.F.M.) can not be satisfied. Therefore, a $J$-integral formulation appropriate for nonlinear elasticity (Crouch and Huang, 1994) is used to characterize the initiation of crack growth in these materials.

*Table 1.* Glass transition temperature, Young's modulus and tensile yield strength of the rubber-modified epoxies used in this study.

| Materials | $T_g^{\mathrm{b}}$ (°C) | $E^{\mathrm{c}}$ (GPa) | $\sigma_y^{\mathrm{c}}$ (MPa) |
|---|---|---|---|
| Epoxy/Rubber: DER 331/pip/CTBN-8 5 phr[a] | $90.7 \pm 0.3$ | $2.89 \pm 0.02$ | $62 \pm 1$ |
| Epoxy/Rubber: DER 331/pip/CTBN-8 10 phr | $89.6 \pm 0.2$ | $2.60 \pm 0.02$ | $57 \pm 1$ |
| Epoxy/Rubber: DER 331/pip/CTBN-8 15 phr | $88.9 \pm 0.2$ | $2.43 \pm 0.03$ | $50 \pm 1$ |
| Epoxy/Rubber: DER 331/pip/CTBN-8 20 phr | $88.5 \pm 0.3$ | $2.24 \pm 0.02$ | $46 \pm 1$ |
| Epoxy/Rubber: DER 331/pip/CTBN-8 25 phr | $88.1 \pm 0.3$ | $1.91 \pm 0.03$ | $39 \pm 1$ |

[a] phr : parts per hundred parts resin by weight.
[b] $T_g$ was determined by differential scanning calorimetry at a heating rate of 10°C/min.
[c] $E$ and $\sigma_y$ were determined by uniaxial tensile test at a strain rate of $2.6 \times 10^{-4}$/sec.

the process zone in the crack wake was demonstrated by experiments in which toughness measurements were made after the crack wake had been removed.

## 2. Experimental

The rubber-modified epoxy polymers used in this work were formed by combining (by weight) 100 parts of a liquid diglycidyl ether of bisphenol-A,[2] 5 parts of curing agent,[3] and 5, 10, 15, 20 and 25 parts of a carboxyl-terminated acrylonitrile-butadiene copolymer.[4] The materials were cured at 120°C for 16 hours in a Teflon®-coated mold. The glass-transition temperature $T_g$, Young's modulus $E$, and tensile yield strength $\sigma_y$, of these epoxies are listed in Table 1. After curing, double-cantilever-beam specimens were machined, as shown in Figure 2. The width $b$ of these samples was 6.35 mm, and the thickness $2h$ was 40 mm. An initial crack was formed by machining a notch of length 35 mm, and then tapping a razor blade into the tip of the notch to form a sharp crack prior to testing. Side grooves of depth 1.27 mm were used to keep the crack in the mid-plane of the samples.

$R$-curve measurements were performed using a screw-driven Instron testing machine with a crosshead speed of 0.5 mm/min. When some crack growth was observed, the specimen was unloaded so as to arrest the crack. This formed a striation on the fracture surface that corresponded to the current position of the crack tip. The sample was then reloaded to induce further crack growth, and unloaded again to mark the new position of the crack tip. This process was repeated until catastrophic crack growth caused failure of the sample. After failure, the fracture surface was examined in an optical microscope, and successive crack lengths were measured from the striations. The toughness $\Gamma$ corresponding to a particular crack length $a$ was determined from the equation (Wiederhorn et al., 1968)

$$\Gamma = \frac{12P^2(a + 0.668h)^2}{b_n E b h^3}, \tag{3}$$

where $P$ is the applied load, $b$ is the specimen width, $b_n$ is the crack width, $E$ is the Young's modulus of the material (given in Table I), and $h$ is the specimen half-thickness. This equation

---

[2] Epoxy DER® 331, produced by the Dow Chemical Co.
[3] piperidine from Aldrich Co.
[4] HYCAR® CTBN 1300 × 8, produced by the B.F. Goodrich Co.

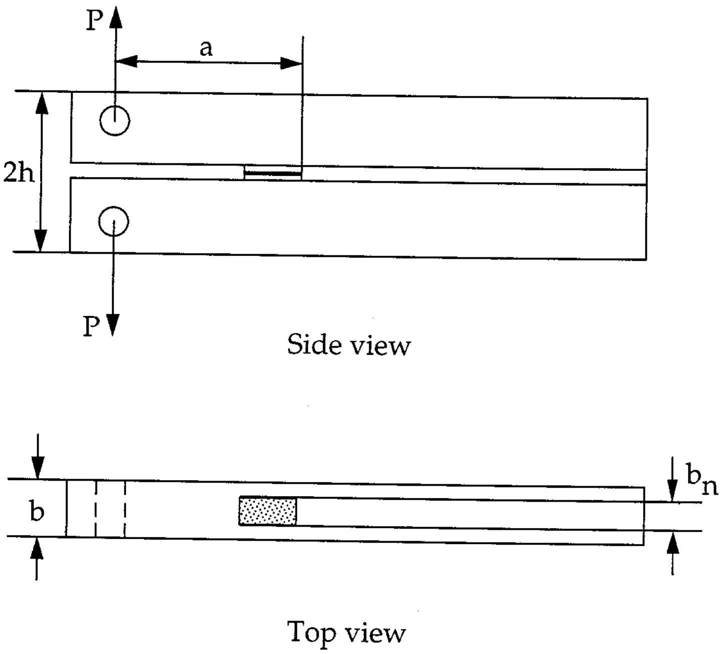

Side view

Top view

*Figure 2.* Diagram of the double-cantilever-beam specimens used in this study. The width, $b$, of these samples was 6.35 mm, and the thickness, $2h$, was 40 mm. An initial crack was formed by machining a notch of length 35 mm, and then tapping a razor blade into the tip of the notch to form a sharp crack prior to testing. Side grooves of depth 1.27 mm were used to keep the crack in the mid-plane of the samples.

is valid when $a/h > 1$ (Wiederhorn et al., 1968). The fracture toughness was then plotted against the corresponding crack extension to establish $R$-curves (Figure 3). It should be noted that $R$-curves could not be obtained for the 5-phr rubber-modified epoxy at the crosshead-displacement rate used, because the crack growth became unstable very soon after initiation.

The evolution of the process zone was studied using a second set of samples tested in an identical fashion. Thin sections at the mid-plane of the samples and perpendicular to the crack surfaces and parallel to the direction of crack propagation were obtained by metallographic thinning techniques (Holik et al., 1979). The cracked region of a specimen was embedded in a clear epoxy resin, and its thickness was reduced by a combination of cutting, grinding and polishing until a final thickness of about 50 $\mu$m was reached. The thinned section was polished to be optically flat by using a series of alumina polishing powders down to a 0.05 $\mu$m grit size. This was then examined using transmitted light in a Nikon research microscope. The process zone appeared dark owing to the increase in light scattering caused by cavitation of the rubber particles and plastic deformation of the surrounding matrix. The resultant TOM micrographs of the process zones for these rubber-modified epoxies are shown in Figure 4. Fracture surfaces were examined by scanning electron microscopy (SEM) (Figure 5).

The effect of the crack wake on toughness was examined by repeating the $R$-curve measurements described above. These new tests were interrupted after a crack growth of about 20 mm, by which time a fully-developed crack wake of uniform thickness had been obtained. A strip of material about 1.5 mm thick was machined off both surfaces of the crack up to about 2 mm or less behind the trace of the crack tip on the side surface of the sample (Figure 6). This process completely removed the crack wake except in a region immediately behind the

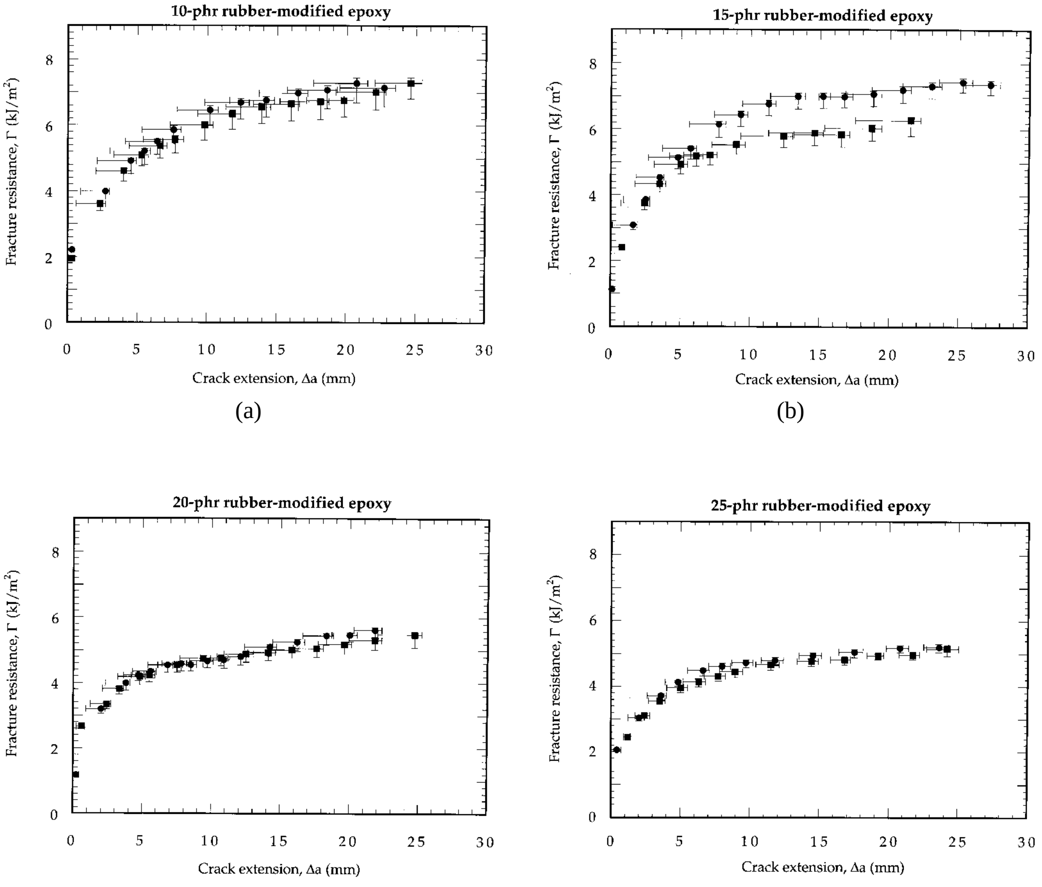

(a) (b)

(c) (d)

*Figure 3.* Experimental $R$-curves for the (a) 10-phr (b) 15-phr (c) 20-phr (d) 25-phr rubber-modified epoxies. The results for two separate specimens of each composition of epoxy are shown and designated by ■ and ●. The ambiguity in the crack extension resulting from the 'thumbnail' shape of the crack is reflected in the error bars.

crack tip. Further crack growth was obtained upon subsequent loading, and a new $R$-curve was established (Figure 7). A linear-elastic finite-element analysis was performed using a commercial package[5] to investigate the possibility that the crack-growth driving force might be affected by the change in geometry associated with removal of material behind the crack. This analysis showed that the crack-growth driving force at a given load level decreases by up to about 15 percent if 10 percent of the material in the arms of the double-cantilever beam is removed. This decrease in the driving force means that the actual drop in toughness is slightly larger than that shown in Figure 7, and is reflected in the error bars of that figure.

---

[5] ABAQUS®, Bibbitt, Karlsson & Sorensen, Inc.

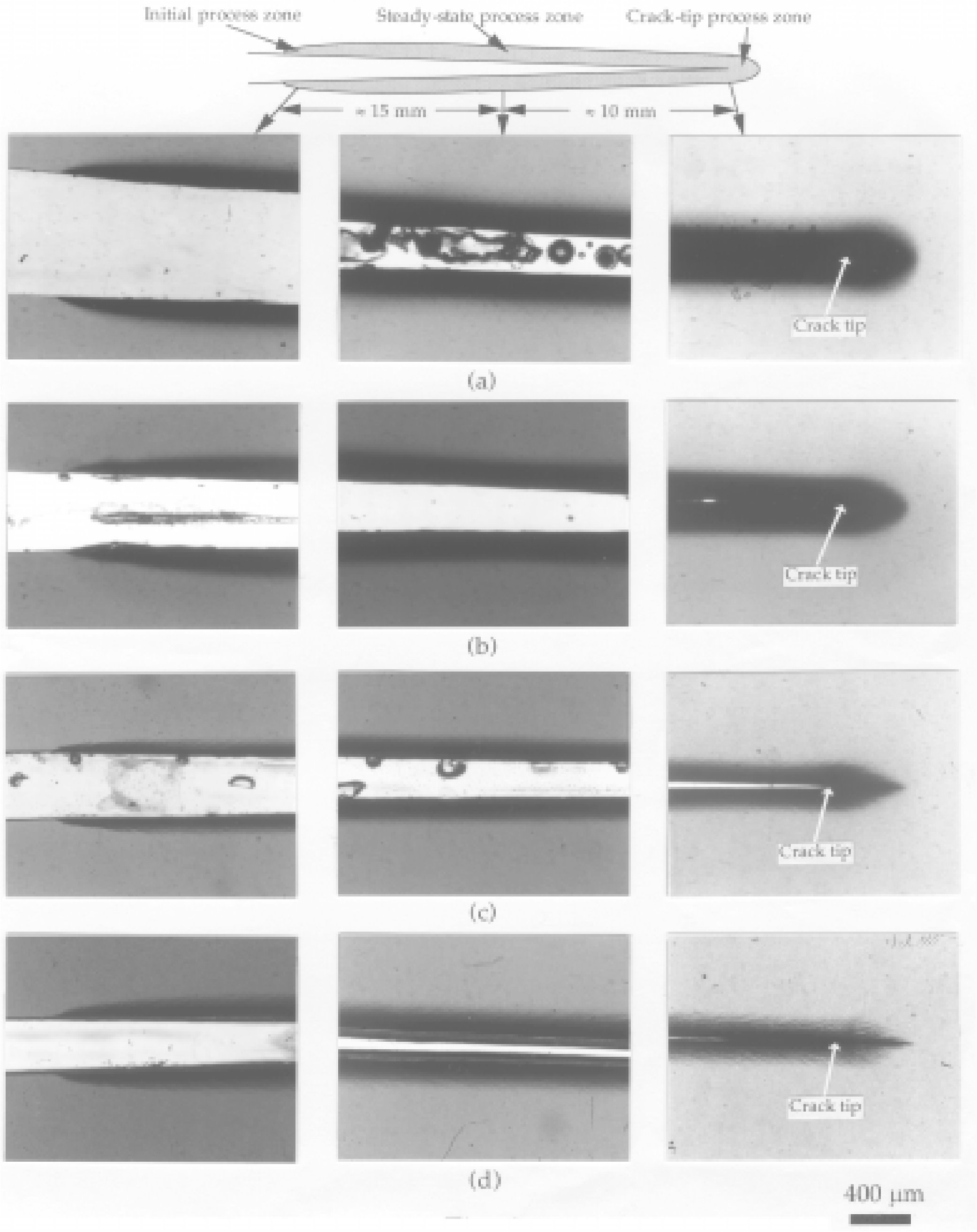

*Figure 4.* Transmission-optical micrographs of the process zone for the (a) 10-phr (b) 15-phr (c) 20-phr (d) 25-phr rubber-modified epoxies. These sections were taken from the mid-section of the samples.

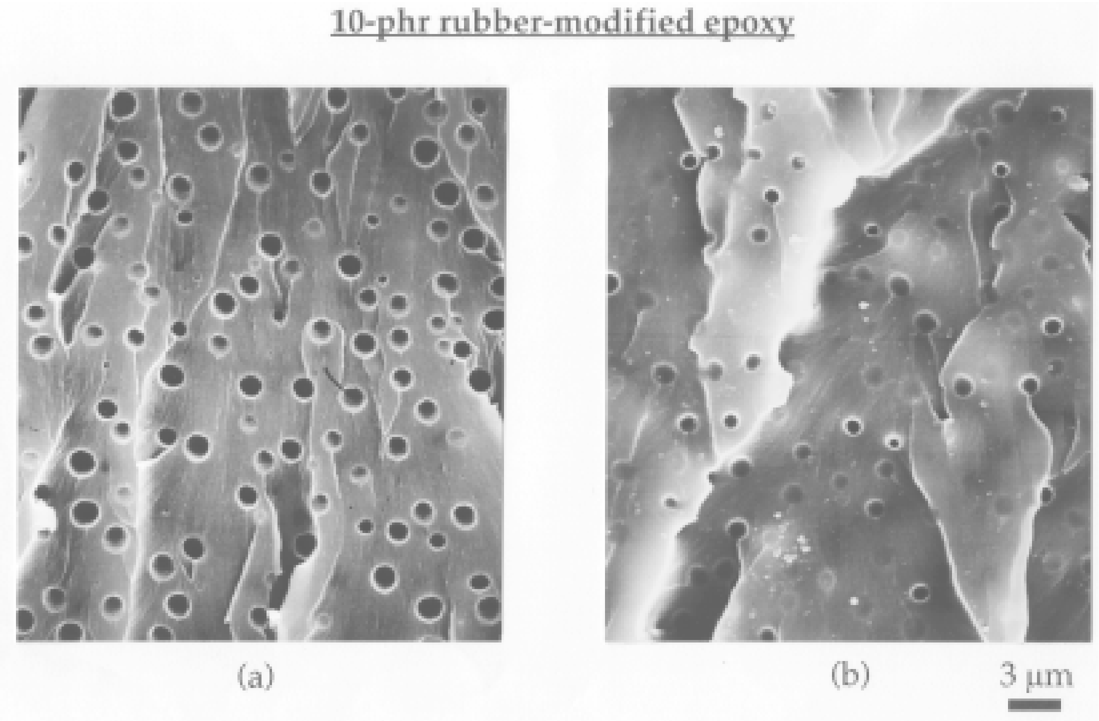

*Figure 5.* Scanning-electron micrographs of (a) steady-state and (b) fast-crack-growth fracture surfaces for the 10-phr rubber-modified epoxy.

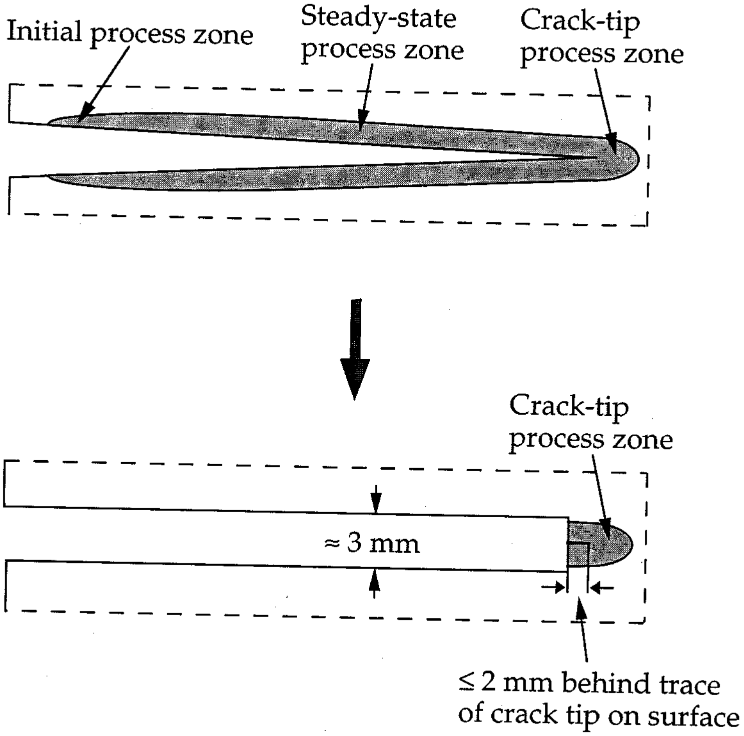

*Figure 6.* Schematic diagram of the removal of the crack wake.

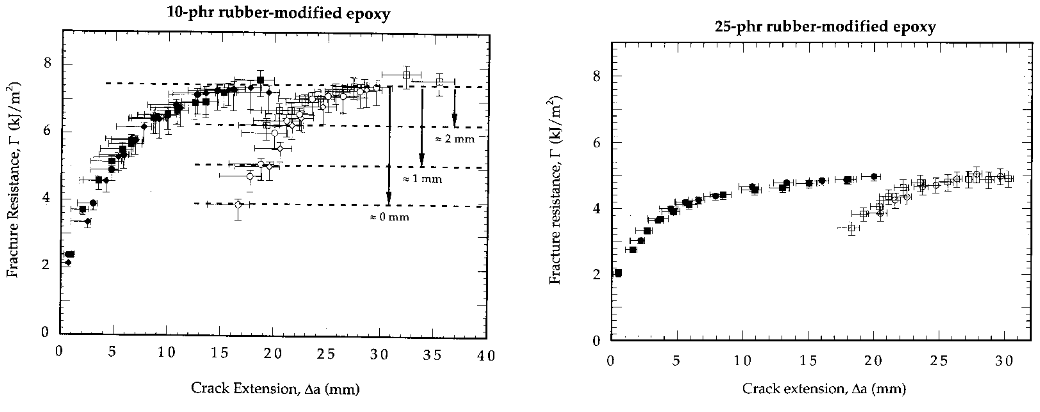

(a) (b)

*Figure 7.* Experimental $R$-curves for two separate samples of (a) 10-phr (b) 25-phr rubber-modified epoxies. The solid symbols (■ and ●) represent the data points obtained *before* the crack wake was removed. The open symbols (□ and ○) represent the data points obtained *after* the crack wake was removed. In (b), the wake was removed up to 2 mm from the trace of the crack on the surface of the sample. In (a), the effect of removing the wake up to 2, 1, and 0 mm from the surface trace is shown.

## 3. Results

### 3.1. CRACK-GROWTH RESISTANCE CURVES

A significant $R$-curve behavior was observed for the 10-, 15-, 20- and 25-phr rubber-modified epoxies (Figure 3). With a crack growth of less than about 1 mm, the fracture resistance was between 1 and 2 kJ/m$^2$ for all the materials. After the crack had grown between 10 and 20 mm, the toughness rose to an approximately steady-state value of about 6–7 kJ/m$^2$ for the 10- and 15-phr rubber-modified epoxies and of about 5–6 kJ/m$^2$ for the 20- and 25-phr rubber-modified epoxies. All the $R$-curve measurements were terminated by the onset of unstable crack growth. This instability was characterized by an abrupt disappearance of the process zone (Figure 8) and by a very high crack velocity. The reason for the instability that leads to catastrophic failure is not understood and needs to be investigated further. It is possibly a visco-elastic effect. However, it is also possible that the microstructural variations in the density of the rubber concentration might be important. In this context, it is perhaps significant that the most dilute (5-phr) rubber-modified epoxy was so prone to unstable crack growth that no portion of the $R$-curve could be obtained, despite the fact that the toughness at which initial crack growth was detected was comparable to the results from the other compositions.

A comparison of the scanning-electron micrographs of the fast-crack-growth fracture surfaces with those of the steady-state fracture surfaces (Figure 5) shows that both the density of cavitation and the void size decreased after the instability occurred. This indicates that both the cavitation rate and the plastic flow in these materials are time-dependent phenomena. This observation was supported by a series of experiments using a 10-phr rubber-modified epoxy in which different cross-head displacement rates were used (between 0.5 and 2 mm/min), and the crack was allowed to grow without being arrested. The crack velocities were monitored using a video camera until the tests were interrupted by the onset of an instability. In all these tests it was observed that the applied crack-driving force increased as a function of crack length

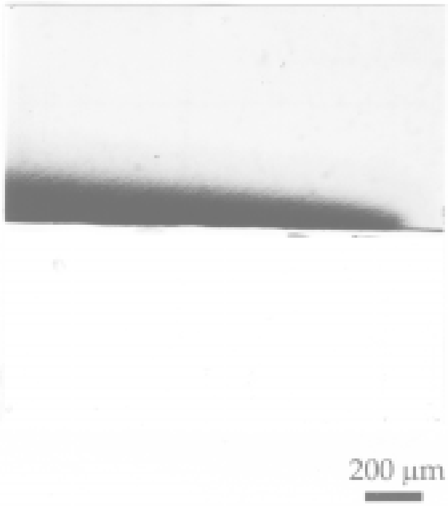

*Figure 8.* Transmission-optical micrograph of the process zone in the region of the crack instability for a 10-phr rubber-modified epoxy.

(i.e., $R$-curve behavior was *always* obtained), but the maximum value was very sensitive to the crack velocity. The crack-driving force never rose above $4\,\mathrm{kJ/m^2}$ for the fastest cracks for which stable crack growth occurred. These cracks had velocities of up to 1 mm/s, and were associated with the higher cross-head displacement rates. This is about a factor of two lower than the highest values of steady-state toughness that was obtained for these materials when fractured under quasi-static conditions.

### 3.2. EVOLUTION OF THE PROCESS ZONE

The features of the experimental $R$-curves, which show a rise in toughness until an approximate steady-state is reached, can be directly correlated to the evolution of the process zone obtained from TOM analyses (Figure 4). In these micrographs, the position of the initial crack tip can be clearly identified since it corresponds to the point from which the process zone appears to evolve. The absence of a process zone behind this location suggests that the process of introducing the initial crack was done at a sufficiently rapid rate to suppress cavitation and void growth. As the crack grew under the applied loading, the process zone moved with it and left a trace of its outer boundary in the crack wake. The round shape of the process zone ahead of the crack is consistent with one associated with dilatation (McMeeking and Evans, 1982). However, there appears to be a transition to a wedge-shaped zone (Rose and Swain, 1988; Yu and Shetty, 1989) at higher rubber concentrations.

It will be observed from Figure 4 that, during the early stage of crack growth, there was an apparent fanning out of the crack wake. This is consistent with prior TOM observations of the process zone developing ahead of the crack tip (Pearson and Yee, 1991). Eventually, the wake reached a uniform width, which implies a steady-state with a process zone of constant size. It does not appear that this steady-state width is significantly larger than the width of the initial zone that develops ahead of the crack before significant growth has occurred. In particular, it should be noted from Figures 3 and 4 that the steady-state toughness was reached at a crack length significantly longer than that required to obtain a process zone of a constant size. This is consistent with the notion that the process zone contributes to the crack-growth resistance as it moves into the wake (Budiansky et al., 1983).

Another important feature observed from Figure 4 is that the size of the steady-state process zone decreased from about 200 $\mu$m for the 10- and 15-phr rubber-modified epoxies to about 150 $\mu$m for the 20- and 25-phr rubber-modified epoxies. This decrease in width appears to correspond with the drop in steady-state toughness noted in Figure 3, and is consistent with micromechanics models of toughening that suggest a linear correlation between the size of the process zone and the toughness (McMeeking and Evans, 1982; Budiansky et al., 1983; Evans and Faber, 1984).

### 3.3. EFFECTS OF THE CRACK WAKE

The contribution of the crack wake to the toughness was investigated by a series of $R$-curve measurements in which a portion of the process zone was removed after an approximate steady-state had been reached (Figure 7). As can be seen from this figure, removing the wake caused a significant drop in the toughness. Further crack growth results in the toughness increasing back up to the original steady-state value. Figure 7(a) demonstrates how the toughness systematically dropped as the amount of the process zone left in the wake of the crack was reduced from 2 mm to 0 mm. It should be noted that, while the extent of the wake that remained was measured relative to the trace of the crack tip on the side surface of the sample, observations of the fracture surface showed that the crack front had a ‘thumbnail’ shape. So, even when the entire wake was nominally removed, up to 3 mm was left undisturbed in the center of the specimen by the machining. Since no portion of the process zone ahead of any segment of the crack tip was removed in these experiments, the results demonstrate unambiguously the contribution of the crack wake to the toughness (despite the absence of any bridging in these materials). This behavior is expected because unloading of material in the process zone as it passes into the wake results in hysteresis losses (Tvergaard and Hutchinson, 1992; McMeeking and Evans, 1982; Evans et al., 1986; Yang, 1991). (Alternatively, it is possible to consider the dilatational characteristics of the cavitation and subsequent void growth within the wake as inducing closing tractions on the crack tip (McMeeking and Evans, 1982)). The removal of this residual deformation (or compression) in the crack wake results in a decrease in the fracture resistance. The technique of removing the process zone has previously been used to show that interlocking grains in the crack wake were the major sources of toughness in polycrystalline alumina (Knehens and Steinbrech, 1982). To the authors’ knowledge, the present work is the first experimental demonstration of the expected result (McMeeking and Evans, 1982) that removing even a non-bridging crack wake lowers the toughness.

## 4. Discussion

Previous measurements of toughness for the 10-phr rubber-modified epoxy gave values of about 1.6 kJ/m$^2$ (Pearson and Yee, 1991; Yee et al., 1993). These observations were obtained from specimens tested in three-point bending subjected to a constant displacement rate. Post-failure examinations showed that the crack had grown by less than 250 $\mu$m before the onset of instability (Pearson and Yee, 1991). Therefore, the measured toughness of 1.6 kJ/m$^2$ is consistent with the curves of Figure 3. Huang and Kinloch (1992) report a value of 5.9 kJ/m$^2$ for the toughness of an epoxy toughened with 15-phr of rubber. This value is close to the steady-state toughness obtained in the present experiments for the 15-phr epoxy. It is somewhat surprising that $R$-curves have not previously been reported for these materials. However, it appears that experiments were often done under conditions in which the crack is continually growing (Bascom et al., 1975; Bascom and Cottington, 1976), rather than under the quasi-static conditions from which the data of Figure 3 were obtained. As mentioned above, the steady-state toughness can be substantially reduced even at moderate crack velocities. Furthermore, when the steady-state toughness is low, other features in the load-displacement plots may command more attention than the details that might indicate $R$-curve bahavior.

The plots of Figures 3 and 7 unambigously demonstrate the existence of an $R$-curve and the influence of the process zone in the wake of a crack. This confirms that *extrinsic* toughening models, as are prevalent in the literature, are appropriate for rubber-modified epoxies. However, the $R$-curves of Figure 3 appear to indicate that initial values of toughness are five to ten times higher than the *intrinsic* toughness of the unmodified epoxy which is about 0.2 kJ/m$^2$ (Pearson and Yee, 1991; Yee et al., 1993). It is possible that the $R$-curves do indeed rise very rapidly from an intrinsic toughness of 0.2kJ/m$^2$, but the resolution of the present experiments (limited to about 1 mm of crack growth) is not sufficient to detect this. Alternatively, it is possible that the presence of the rubber particles affect the intrinsic toughness of the material. For example, the structure of the epoxy matrix may, perhaps, be modified by the processing required to introduce the rubber particles. It should also be noted that when a crack extends it intercepts rubber particles. Within the framework of a micro-mechanics approach to toughening brittle materials, the energy associated with debonding or fracture of the rubber in the plane of the crack would then be properly considered to contribute to the *intrinsic* toughness.

In the review stage of this manuscript, it was suggested that the results presented here were purely an artifact of an increasing nonlinear zone developing ahead of the crack, leading to a violation of L.E.F.M. conditions. In response to this comment, it should be emphasized that the macroscopic deformations of these specimens were dominated by linear elasticity and, therefore, L.E.F.M. is indeed an appropriate tool with which to describe the fracture of these specimens. This was verified by monitoring the crack-opening displacement as the crack grew, and as the sample was loaded and unloaded. During loading, a deviation from linearity in the load-displacement curve was observed. That this was associated with a compliance change caused by crack growth was verified by observing that unloading from the point at which the non-linearity was first observed resulted in no permanent deformation. After about 15 mm of crack growth, unloading resulted in a residual opening of about 5 percent of the maximum opening under load. However, this is expected with a process zone in which there is a volume expansion associated with cavitation. The increased volume of the process zone wedges open the crack. (Conversely, one can consider that the reaction force supplied by the matrix compresses the process zone and acts to close the crack – shielding is one way of viewing the toughening process.) In one set of experiments, the residual crack opening was measured in a microscope and then monitored as the process zone was removed by machining (Figure 6). Ninety percent of the residual displacement was recovered by removing the entire wake up to the surface of the crack tip. The final 10 percent was recovered when the process zone immediately ahead of the crack tip was removed. In other words, the portion of the process zone immediately ahead of the crack tip was responsible for less than a 0.5 percent deviation from linear-elasticity in these samples. This appears to be a compelling case for arguing that L.E.F.M. is an appropriate tool for describing the fracture of these materials.

The question of whether these results were obtained under plane-strain conditions was also raised in the review process. Plane-strain conditions are required before one can quote a toughness value as being a geometry-independent quantity. Macroscopic deformations can be dominated by linear elasticity (i.e., the test is a valid L.E.F.M. test), but the specimen can be sufficiently thin that plane-strain conditions do not prevail at the crack tip. Under these conditions, the size of the process zone *may* depend on the specimen thickness, and the toughness *may* also vary with thickness. However, the basic physics and mechanics of the problem remain unchanged. The conditions for strict plane-strain conditions are that the plastic zone size should be less than about 1/25 of the specimen thickness. An approximate expression for the scale of the non-linear process zone ahead of the crack, $R_0$ is given by (Tvergaard and Hutchinson, 1992)

$$R_0 = \frac{1}{3\pi}\frac{E\Gamma_0}{(1-\nu^2)\sigma_c^2}, \tag{4}$$

where $\sigma_c$ is the critical stress required to induce nonlinear deformations. Setting this equation to 1/25 of the specimen thickness $b$ gives the well-known result for strict plane-strain conditions to apply:[6]

$$b \geqslant 2.5\frac{E\Gamma_0}{(1-\nu^2)\sigma_c^2}. \tag{5}$$

Given the uncertainty in both $\Gamma_0$ and $\sigma_c$, it seems better to compare the experimentally measured size of the process zone with the thickness, rather than use Eqn. (5). Because of the exothermic reaction that accompanies curing, the thickness of these samples was limited to about 6.4 mm. The size of the process zone is between 150 and 220 $\mu$m. This corresponds to a ratio of between 29:1 and 40:1 - more than ample for strict plane-strain conditions. However, in order to get long crack extensions without the crack leaving the center plane, it was necessary to introduce side grooves. This does reduce the ratio of the process-zone size to the thickness down to between 17:1 and 25:1. However, it should be noted that tests without this side groove (using the full 6.4 mm thickness of the samples) showed very similar results, except the crack left the mid-plane before catastrophic failure interrupted the tests (therefore, a large region of steady-state crack growth was not so readily obtained). In particular, there seemed to be no indication that the side-groove affected the toughness values or the $R$-curves. Furthermore, a section taken across the crack plane confirmed that the region affected by the free surface was limited to a relatively small area (Figure 9), and there was no obvious change in failure mode near the free surface (also confirmed by observations of the fracture surface). It therefore seems reasonable to conclude that the results are dominated by plane strain conditions, and certainly much more sensitive to rate effects than to any details of the geometry.

## 5. Concluding remarks

A significant $R$-curve behavior was observed for DGEBA epoxies toughened by different volume fractions of CTBN rubbery phase. For these rubber-modified epoxies, the toughness

---

[6] This is often expressed as $b \geqslant 2.5(K_{\mathrm{I}c}/\sigma_c)^2$. It is important to appreciate that here, $K_{\mathrm{I}c}$ is the critical mode-I plane-strain stress-intensity factor required to initiate fracture. The size of the process zone is determined by the crack-tip stresses at the point at which the crack just grows. Therefore, this equation contains a term representing the intrinsic toughness of the material (the strain-energy release rate acting on the tip of the crack) rather than the toughness measured by external observer (the applied strain-energy release rate at fracture).

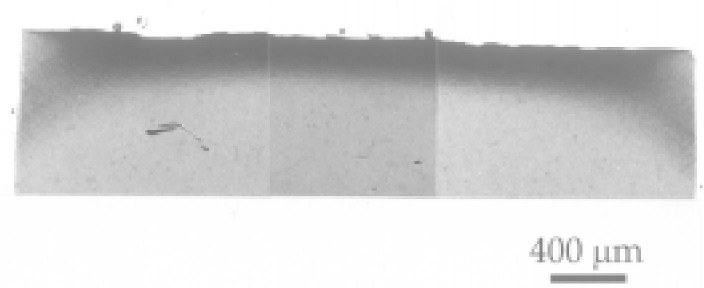

*Figure 9.* Transmission-optical micrograph of a section perpendicular to the direction of crack propagation for a 10-phr rubber-modified epoxy showing the limited extent of the plane-stress region.

rose to an approximately steady-state value of between 5 and 7 kJ/m$^2$ after a crack growth of between 10 and 20 mm. These features of the experimental $R$-curves were directly correlated to the evolution of the process zone to a steady-state crack wake of constant thickness. A significant contribution to toughening from the crack wake, despite the absence of bridging, was demonstrated by measuring the toughness after the crack wake had been removed. These experiments showed that the fracture resistance dropped substantially upon removal of the wake. The toughness rose back to the steady-state value upon further crack growth and re-development of the wake.

The behavior described in this paper is consistent with several analyses of toughening of rubber-modified polymers in which the toughness is assumed to derive only from the nonlinear, irreversible deformation of material as it passes through the process zone and into the crack wake. Provided the constitutive properties of the material are known, these analyses provide an approach by which one could calculate the evolution of the $R$-curve and the steady-state toughness. The full realization of the $R$-curve is crucial to ensure that the ultimate toughenability, i.e., the steady-state toughness, is achieved (Mai and Lawn, 1986; Cook and Clarke, 1988). Less than optimal strengths will result from the premature unstable crack growth caused by the loading geometry, compliance of the material, or rate effects.

## Acknowledgments

This work is supported by the National Science Foundation under grant # CMS-9523078. The authors are thankful to Dr. J. Huang for his valuable help and discussions, and to P.C. Niven for his experimental help.

## References

Bascom, W.D., Cottington, R.L., Jones, R.L. and Peyser, P. (1975). The fracture of epoxy- and elastomer-modified epoxy polymers in bulk and as adhesives. *Journal of Applied Polymer Science* **19**, 2545–2562.

Bascom, W.D. and Cottington, R.L. (1976). Effects of temperature on the adhesive fracture behavior of an elastomer-epoxy resin. *Journal of Adhesion* **7**, 333–346.

Budiansky, B., Hutchinson, J.W. and Lambrapolous, J.C. (1983). Continuum theory of dilatant transformation toughening in ceramics. *International Journal of Solids and Structures* **19**, 337–355.

Cook, R.F. and Clarke, D.R. (1988). Fracture stability, $R$-curves and strength variability. *Acta Metallurgica* **36**, 555-562.

Crouch, B.A. and Huang, D.D. (1994). The $J$-integral technique applied to toughened nylons under impact loading. *Journal of Material Science* **29**, 861–864.

Evans, A.G. and Faber, K.T. (1984). Crack-growth resistance of microcracking brittle materials. *Journal of American Ceramic Society* **67**, 255–260.

Evans, A.G., Ahmad, Z.B., Gilbert, D.G. Gilbert, and Beaumont, P.W.R. (1986). Mechanisms of toughening in rubber-toughened polymers. *Acta Metallurgica* **34**, 79–87.

Hashemi, S. and Williams J.G. (1991). Single and multi-specimen $R$-curve methods for $J_{IC}$ determination of toughened nylons. *Journal of Materials Science* **26**, 621–630.

Holik, A.S., Kambour, R.P., Hobbs, S.Y. and Fink, D.G. (1979). Grinding and polishing techniques for thin sectioning of polymeric materials for transmission light microscopy, *Microstructural Science* **7**, 357–367.

Huang, Y. and Kinloch, A.J. (1992). Modelling of the toughening mechanisms in rubber-modified epoxy polymers. Part II: A quantitative description of the microstructure-fracture property relationships. *Journal of Materials Science* **27**, 2763–2769.

Kinloch, A.J. and Guild, F.J. (1996). Predictive modeling of the properties and toughness of rubber-toughened epoxies. (Edited by C.K. Riew and A.J. Kinloch), *Toughened Plastics II: Novel Approaches in Science & Engineering*, American Chemical Society, Washington, D.C.

Kinloch, A.J., Shaw, S.J., Tod, D.A. and Hunston, D.L. (1983a). Deformation and fracture behavior of a rubber-modified epoxy: 1. Microstructure and fracture studies. *Polymer* **24**, a 1341–1354.

Kinloch, A.J., Shaw, S.J. and Hunston, D.L. (1983b). Deformation and fracture behavior of a rubber-modified epoxy: 2. Failure criteria. *Polymer* **24**, b 1355–1363.

Knehens, R. and Steinbrech, R. (1982). Memory effect of crack resistance during slow crack growth in notched $Al_2O_3$ bend specimen. *Journal of Materials Science Letters* **1**, 327–329.

Kunz-Douglass, S., Beaumont, P.W.R. and Ashby, M.F. (1980). A model for the toughness of epoxy-rubber particulate composites. *Journal of Materials Science* **15**, 1109–1123.

Mai, Y.-W. and Lawn, B.R. (1986). Crack stability and toughness characteristics in brittle materials. *Annual Reviews of Materials Science* **16**, 415–439.

Marshall, D.B. and Swain, M.V. (1988). Crack resistance curves in magnesia-partially stabilized zirconia. *Journal of American Ceramic Society* **71**, 399–407.

McMeeking, R.M. and Evans, A.G. (1982). Mechanics of transformation toughening in brittle materials. *Journal of American Ceramic Society* **65**, 242–246.

Pearson, R.A. and Yee, A.F. (1986). Toughening mechanisms in elastomer-modified epoxies Part II: Microscopy studies. *Journal of Materials Science* **21**, 2475–2488.

Pearson, R.A. and Yee, A.F. (1991). Influence of particle size and particle-size distribution on toughening mechanisms in rubber-modified epoxies. *Journal of Materials Science* **26**, 3828–3844.

Rice, J.R. (1968). A path independent integral and the approximate analysis of strain concentration by notches and cracks. *Journal of Applied Mechanics* **35**, 379–386.

Rose, L.R.F. and Swain, M.V. (1988). Transformation zone shape in ceria-partially-stabilized zirconia. *Acta Metallurgica* **36**, 955–962.

Swain, M.V. and Hannink, R.J.H. (1984). $R$-Curve behavior of zirconia ceramics. (Edited by N. Claussen, M. Rühle and A.H. Heuer), *Advances in Ceramics, Vol. 12, Science and Technology of Zirconia II*. American Ceramic Society, Colombus, OH pp.225–240.

Swanson, P.L., Fairbanks, C.J., Lawn, B.R., Mai, Y.-W. and Hockey, B.J. (1987). Crack-interface grain bridging as a fracture-resistance mechanism in ceramics: I. Experimental study on alumina. *Journal of American Ceramic Society* **70**, 279–289.

Tvergaard, V. and Hutchinson, J.W. (1992). The relation between crack growth resistance and fracture process parameters in elastic-plastic solids. *Journal of the Mechanics and Physics of Solids* **40**, 1377–1397.

Wiederhorn, S.M., Shorband, A.M. and Moses, R.L. (1968). Critical analysis of the theory of the double cantilever method of measuring fracture-surface energies. *Journal of Applied Physics* **39**, 1569–1572.

Yee, A.F. and Pearson, R.A. (1986). Toughening mechanisms in elastomer-modified epoxies Part I: Mechanical studies. *Journal of Materials Science* **21**, 2462–2474.

Yee, A.F., Li, D. and Li, X. (1993). The importance of constraint relief caused by rubber cavitation in the toughening of epoxy. *Journal of Materials Science* **28**, 6392–6398.

Yu, C.-S. and Shetty, D.K. (1989). Transformation zone shape, size and crack-growth-resistance ($R$-Curve) behavior of ceria-partially-stabilized zirconia polycrystals. *Journal of American Ceramic Society* **72**, 921–928.

Yang, W, (1991). Toughness increment by crack growth in toughened structural materials. *Acta Mechanica Sinica* **7**, 131–1139.

Zhou, Z., Landes, J.D. and Huang, D.D. (1994). $J$-$R$ Curve calculation with the normalization method for toughened polymers. *Polymer Engineering and Science* **34**, 128–134.